BIOCHEMISTRY
including biophysical chemistry & molecular biology

Article

pubs.acs.org/biochemistry

Mutagenesis and Computational Modeling of Human G-Protein-Coupled Receptor Y2 for Neuropeptide Y and Peptide YY

Bo Xu,[†] Helena Fällmar,[†] Lars Boukharta,[‡] Jasna Pruner,[†] Ingrid Lundell,[†] Nina Mohell,[†] Hugo Gutiérrez-de-Terán,[‡,§] Johan Åqvist,[‡] and Dan Larhammar*,[†]

[†]Department of Neuroscience, Science for Life Laboratory, Uppsala University, Box 593, SE-751 24 Uppsala, Sweden

[‡]Department of Cell and Molecular Biology, Uppsala University, Box 596, SE-751 24 Uppsala, Sweden

[§]Fundación Pública Galega de Medicina Xenómica, Hospital Clínico Universitario de Santiago, E-15706 Santiago de Compostela, Spain

ABSTRACT: Neuropeptide Y and peptide YY receptor type 2 (Y2) is involved in appetite regulation and several other physiological processes. We have investigated the structure of the human Y2 receptor. Computational modeling of receptor−agonist interactions was used as a guide to design a series of receptor mutants, followed by binding assays using full-length and truncated peptide agonists and the Y2-specific antagonist BIIE0246. Our model suggested a hydrogen bond network among highly conserved residues Thr2.61, Gln3.32, and His7.39, which could play roles in ligand binding and/or receptor structure. In addition, the C-terminus of the peptide could make contact with residues Tyr5.38 and Leu6.51. Mutagenesis of all these positions, followed by binding assays, provides experimental support for our computational model: most of the mutants for the residues forming the proposed hydrogen bond network displayed reduced peptide agonist affinities as well as reduced hPYY3-36 potency in a functional assay. The Ala and Leu mutants of Gln3.32 and His7.39 disrupted membrane expression of the receptor. Combined with the modeling, the experimental results support roles for these hydrogen bond network residues in peptide binding as well as receptor architecture. The reduced agonist affinity for mutants of Tyr5.38 and Leu6.51 supports their role in a binding pocket surrounding the invariant tyrosine at position 36 of the peptide ligands. The results for antagonist BIIE0246 suggest several differences in interactions compared to those of the peptides. Our results lead to a new structural model for NPY family receptors and peptide binding.

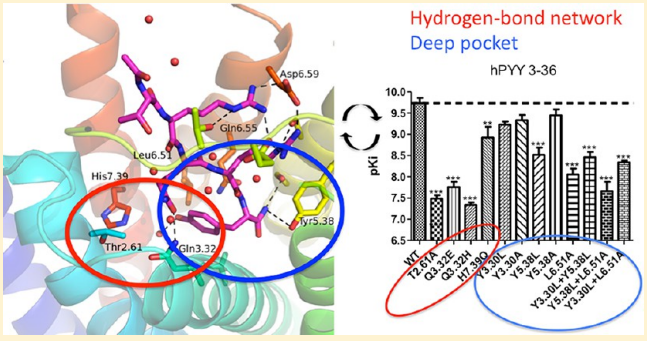

The neuropeptide Y (NPY) system of neuronal and endocrine peptides and receptors has broad biological functions and is involved in several diseases, such as obesity and cancer.[1] However, until now, no effective drugs have been developed for the NPY system,[1−3] an endeavor that could be potentially assisted by studies of peptide−receptor interactions. The NPY family of peptides is in mammals comprised of three related peptides, NPY, peptide YY (PYY), and pancreatic polypeptide (PP), which are 36 amino acids long with a C-terminal amidated conserved tyrosine.[4] The peptides activate receptors that belong to the family of rhodopsin-like (class A) G-protein-coupled receptors (GPCRs). Four functional receptors named Y1, Y2, Y4, and Y5 exist in humans,[5] and additional receptors (Y6−Y8) are present in some other vertebrate lineages.[5−8] The Y6 gene is a pseudogene in humans,[9] whereas Y7 and Y8 have been lost in the lineage leading to mammals.[6,7]

Each of the four human NPY family receptors has a unique peptide binding profile. Two of the most prominent differences are that Y2 can respond to truncated forms of both NPY and PYY, i.e., residues 3−36 and 13−36,[10] and that PP preferentially binds to Y4.[11−14] Nevertheless, all three native peptides, which share a considerable degree of homology, in particular in the C-terminal part, show some affinity for all four receptors.[15] This somewhat promiscuous ligand−receptor behavior has driven the search for highly selective antagonists that can be used as tools for pharmacological characterization of the receptor subtypes and therapeutically for the treatment of, for instance, obesity.[16] The first successful Y2 antagonist developed was BIIE0246,[17] which has become the reference antagonist in Y2 binding studies. Since then, additional antagonists have been reported, with lower molecular weights and the ability to cross the blood−brain barrier,[18−20] which gives them potential therapeutic interest.

One feature that makes the NPY receptor family particularly interesting and suitable for mutagenesis studies is the fact that the three receptors (Y1, Y2, and Y5) are only approximately 30% identical for each pairwise comparison[21] and nevertheless

Received: June 27, 2013
Revised: October 11, 2013
Published: October 11, 2013

can respond to both NPY and PYY. A few mutagenesis studies have been reported for the human Y1 (hY1) receptor, but several discrepancies exist among these.[22−27] There are four published mutagenesis studies of hY2 addressing in total 14 residues.[28−31] Several Y1 and Y2 receptor structural models have been proposed.[23,24,26,31] However, all of these models must be reconsidered in light of the recently determined GPCR structures,[32] which can be used as better starting points for homology-based models that are subsequently tested using mutagenesis and binding studies.

The docking hypothesis for NPY family receptors presented in ref 31 suggested that the conserved Asp6.59 residue in receptors Y1/Y4 and Y2/Y5 interacts in a subtype-specific manner with the two conserved arginines in NPY, i.e., Arg35 and Arg33, respectively. Our previous mutagenesis studies of the hY1 and hY2 receptors identified several positions that are important for the pharmacology of each subtype, but surprisingly, the mutations of the corresponding positions rarely display the same level of importance in Y2 as in Y1.[26,28,29] Here we describe a new computational model of the hY2 receptor and its interactions with native agonists. On the basis of this model, mutagenesis studies of six new positions in hY2, including double mutants, made it possible to validate and propose an improved three-dimensional model of the receptor with new implications for native peptide binding.

MATERIALS AND METHODS

Numbering and Nomenclature Used for Peptides and for Receptor Residues and Mutants. Amino acid positions in peptides are named using the single-letter amino acid abbreviations followed by the sequence correlative number. Receptor residues are named using the three-letter amino acid abbreviations and are numbered according to the system of Ballesteros and Weinstein.[33] Mutants are named with single-letter abbreviations for the wild-type (WT) residue followed by the Ballesteros−Weinstein number and the introduced amino acid.

Computational Modeling. Two protocols were followed in this study. (1) A docking procedure was used to obtain a hY2−hNPY complex that guided the site-directed mutagenesis studies. (2) A hY2 homology model was built in light of novel receptor structure templates. This last model was used for further interpretation of the binding and site-directed mutagenesis results reported herein. The methods followed in each protocol are outlined below.

Docking of hNPY in an Initial Model of the hY2 Receptor. In a previous study, we reported a three-dimensional (3D) model of hY2, which was built using Modeler on the basis of its homology with the human adenosine receptor, hA_{2A} [Protein Data Bank (PDB) entry 3EML].[34] This structure, obtained as described in detail in ref 29, was used here as a starting point for docking the hNPY peptide using the following stepwise docking protocol.

Step 1. First, automated docking of the conserved C-terminal dipeptide fragment of the natural agonists with an acetylated N-terminus [$CH_3C(O)$-R35-Y36-NH_2] was performed using GOLD version 4.0[35] with the Chemscore scoring function,[36] default genetic search parameters, and 50 docking runs. The binding site was defined within a 25 Å radius sphere centered between Thr2.61 and Gln6.55. Such a sphere comprised the entire orthosteric binding cavity between the extracellular loops and TM helices of the model. Docking solutions were clustered according to a 5 Å root-mean-square deviation cluster limit using complete linkage hierarchical clustering.

Step 2. The 36-residue hNPY peptide was built by homology modeling starting from the crystal structure of the avian pancreatic peptide (aPP, PDB entry 2BF9, 53% identical sequence)[37] using Modeler.[38] Fifteen models were generated, and the best model was selected according to the DOPE-HR scoring function.[39] The protein−protein docking program HADDOCK[40] was employed to elucidate the mode of binding of the hNPY peptide to hY2. HADDOCK is a docking method that has demonstrated very good performance in several CAPRI competitions on protein−protein docking predictions.[41] Basically, the docking algorithm is driven by (experimental) knowledge, in the form of information about the interface region between the molecular components and/or their relative orientations. The information used in this work to bias the docking was derived from experimental mutagenesis data,[28,31] as well as from the docking results of the dipeptide obtained with GOLD. Briefly, the user must define a set of residues in each protein, which are thought to directly participate in the protein−protein interaction, termed "active residues". Thereafter, a list of "passive residues" is elaborated as the solvent accessible residues surrounding the active residues, identified with NACCESS,[42] followed by a manual assessment to eliminate membrane-surrounded residues. A set of "ambiguous distance restraints" is thus created, between all active residues of one protein and all active and passive residues of the other. During the docking search, an energy penalty is assigned if an active residue is not contacting any active or passive residue on the partner molecule. It is important to note here that no specific pair interaction is imposed or restrained. Simply, the so-defined active residues in one partner should make contact with at least one of the active or passive residues in the other partner. The docking protocol consists of three stages, namely, a rigid-body energy minimization, a semiflexible refinement in torsion angle space, and a final refinement in explicit solvent. A set of 2000 docking runs was queried for the first phase. The best 200 structures were retained for subsequent refinement. We selected dimethyl sulfoxide as the explicit solvent model, because it better represents the physiological lipophilic environment of membrane proteins (A. Bonvin, personal communication).

Modeling of hY2 Based on the NTSR1 Template. A second version of the 3D model of hY2 was built using the following computational protocol.

Step 1. Human Y1, Y2, Y4, and Y5 protein sequences were downloaded from the Essembl database.[43] The multiple-sequence alignments of these sequences were made with Jalview using default settings of the ClustalW multiple-sequence alignment function.[44]

Step 2. The sequence of the recently crystallized rat neurotensin receptor 1 (NTSR1) was extracted from the corresponding PDB entry 4GRV[45] and aligned with the family alignment of NPY receptors described above. A pairwise hY2-rNTSR1 was obtained and manually curated, in particular for the longer loops, by considering the sequence conservation within the NPY receptor family. The N-terminus was discarded from hY2 modeling because of a lack of similarity.

Step 3. Homology modeling was performed using Modeler,[38] generating 1000 initial homology models. A candidate model was selected on the basis of a low DOPE-HR assessment score[39] and the orientation of Asp6.59 toward the binding

crevice, a highly conserved residue shown to be important by mutagenesis.[31]

Step 4. Automated docking of the NPY/PYY C-terminal pentapeptide [$CH_3C(O)$-T32-R33-Q34-R35-Y36-NH_2] was achieved by means of the Induced Fit Docking protocol[46] in Schrödinger Suite 2011 (Schrödinger LCC, New York, NY). Default settings were used in an enclosing box comprising the entire orthosteric binding cavity between the extracellular loops and TM helices of the model.

Step 5. Molecular dynamics (MD) equilibration was performed on the protein−peptide complex, following the MD protocol for GPCRs as implemented with the GPCR-ModSim web server.[47] Briefly, the complex is automatically embedded in a pre-equilibrated POPC (1-palmitoyl-2-oleoyl-phosphatidylcholine) membrane model, so that the TM bundle is parallel to the vertical axis of the membrane. The system is then soaked with bulk water and inserted into a hexagonal prism-shaped box that is energy-minimized. Then follows a careful equilibration protocol using PBC (periodic boundary conditions) for 2.5 ns, where positional restraints in protein and peptide heavy atoms are gradually released from 1000 to 200 kJ mol^{-1} $Å^{-2}$, followed by a 2.5 ns run in which the soft positional restraint is applied only in the C-alpha trace of the protein.

Step 6. Manual docking of the full NPY peptide was performed with Schrödinger Suite 2011 (Schrödinger LCC). The fragment with the defined secondary structure of the NPY peptide (residues 1−31) was attached to the equilibrated pose of the ^{32}TRQRY^{36}-HN_2 C-terminal fragment with Maestro, followed by 1000 steps of energy minimization with Macromodel in which the secondary structure of peptide and protein was preserved with positional constraints.

Site-Directed Mutagenesis. The QuikChange II site-directed mutagenesis kit (Stratagene, La Jolla, CA) was used to generate the mutants according to the manufacturer's protocol. Briefly, the mutations were introduced via polymerase chain reaction with primers specifically designed for each mutation. A pcDNA-DEST47 vector (Invitrogen, Carlsbad, CA) with a wild-type human Y2 (WT hY2) receptor coding region inserted was used as the parental template.[29] After the generated plasmids had been cloned, the coding regions of the mutants were fully sequenced to confirm the introduced mutation. Upon confirmation of the sequence, plasmids were purified by PureLink HiPure Plasmid DNA purification kits (Invitrogen) for transfection. The following mutants were created: T2.61A, Q3.32E, Q3.32H, Q3.32L, Q3.32A, H7.39Q, H7.39L, H7.39A, Q3.32H+H7.39Q, Y3.30L, Y3.30A, Y5.38L, Y5.38A, L6.51A, Y3.30L+Y5.38L, Y5.38L+L6.51A, Y3.30L+ L6.51A, Q6.55L, and Q6.55N.

Transfection for Transient Receptor Expression. Lipofectamine 2000 transfection reagent (Invitrogen) and Opti-Mem medium (Invitrogen) were used to transfect human embryonic kidney (HEK) 293 cells at 90−95% confluence, with the WT hY2 plasmid and the plasmids for the hY2 mutants according to the manufacturer's instructions. After transfection, the cells were allowed to grow for 72 h in DMEM (Invitrogen) with 10% (v/v) fetal calf serum (Invitrogen), penicillin-streptomycin (Gibco), and amphotericin B (Invitrogen). Thereafter, the cells were washed with phosphate-buffered saline (PBS) twice and scraped off the plate. After centrifugation, the cell pellet was resuspended in binding buffer [25 mM 4-(2-hydroxyethyl)-1-piperazineethanesulfonic acid (Hepes) buffer (pH 7.4) containing 2.5 mM $CaCl_2$ and 1.0 mM $MgCl_2$], and aliquots were stored at −20 °C for binding assays. The protein concentrations of the cell batches were determined using the Bio-Rad Protein Assay (Bio-Rad, Hercules, CA) with bovine serum albumin as a standard.

Binding Assays. The radioligand used was [^{125}I]pPYY with a specific activity of 2200 Ci/mmol (PerkinElmer, Waltham, MA). Human PYY3-36 (Bachem, Bubendorf, Switzerland) and the Y2-specific nonpeptide antagonist BIIE0246 (Boehringer Ingelheim, Ingelheim, Germany) were used for competition assays.

The binding assays were performed according to a previous description with minor changes[28] to determine the K_d values of the radioligand for the different mutants and K_i values for human PYY3-36 and BIIE0246. The cell aliquots were diluted in binding buffer with additional 2 g/L bacitracin. Final volumes of 200 and 100 μL were used for the saturation and competition assay, respectively, and all assays were incubated at room temperature for 3 h. The binding assays were performed in triplicate and repeated independently at least three times.

Functional Assays. The functional inositol phosphate (IP) assay was performed by cotransfection of each receptor construct with a chimeric G protein contruct. The chimeric G-protein (kindly provided by E. Kostenis), with the last four amino acids replaced by the corresponding amino acids from Gαi, can change a Gαi signal transduction pathway to the Gαq pathway, leading to IP generation.[48]

HEK 293 cells (∼90−95% dense) were cotransfected with mutant plasmid constructs and the chimeric G-protein Gαqi4 plasmid using Lipofectamine 2000 (Invitrogen) according to the manufacturer's instructions. Myo[2-^{3}H]inositol (PerkinElmer) at 3 μCi/mL was added on the following day. The day after, the cells were detached with a PBS/EDTA mixture (0.2 g/L) and resuspended in assay buffer containing 10 mM LiCl (20 mM Hepes, 137 mM NaCl, 5 mM KCl, 0.44 mM KH_2PO_4, 4.2 mM $NaHCO_3$, 1.2 mM $MgCl_2$, 1 mM $CaCl_2$, and 10 mM glucose). The cells were preincubated for 10 min and then stimulated with serial dilution of hPYY3-36 for 20 min at 37 °C. An equal volume of ice-cold 0.8 M perchloric acid was added and incubated on ice for 60 min to lyse the cells. The reaction was terminated by neutralization with $KOH/KHCO_3$. The generated [^{3}H]inositol phosphates were isolated by ion exchange chromatography on AG 1-X8 resin (Bio-Rad). The resin was washed with 5 mM Na_2B_4 and 60 mM NH_4-formate and eluted with 1 M NH_4 formate and 0.1 M formic acid (method adapted from ref 49). After the sample had been mixed with OptiPhase HiSafe (PerkinElmer), the ^{3}H radioactivity was measured with a liquid scintillation counter. The assay was performed in triplicate for each concentration.

Data Analysis. Prism 5.0 (GraphPad Software, La Jolla, CA) was used to analyze the binding and IP assay results. Results from the saturation, competition, and IP assays were analyzed by nonlinear regression curve fitting. Scatchard transformation for saturation assays was analyzed by linear regression. Hill slope values were calculated for all individual competition assays. In addition, the curves were fit a with one-site binding model to calculate the K_i values for WT hY2 and all mutants. One-way analysis of variance (ANOVA) with a Dunnett's post test was performed for statistical analysis of the pK_d, pK_i, and pEC_{50} values, which represent −log values of K_d, K_i, and EC_{50}, respectively.

Detection of Receptor Expression. Coverslips coated with 0.1 mg/mL poly-D-lysine were seeded with HEK 293 cells transiently expressing WT hY2 or mutant receptors. Cells were grown for 48 h at 37 °C in 5% CO_2. Similarly, the cells were

dx.doi.org/10.1021/bi400830c | Biochemistry 2013, 52, 7987−7998

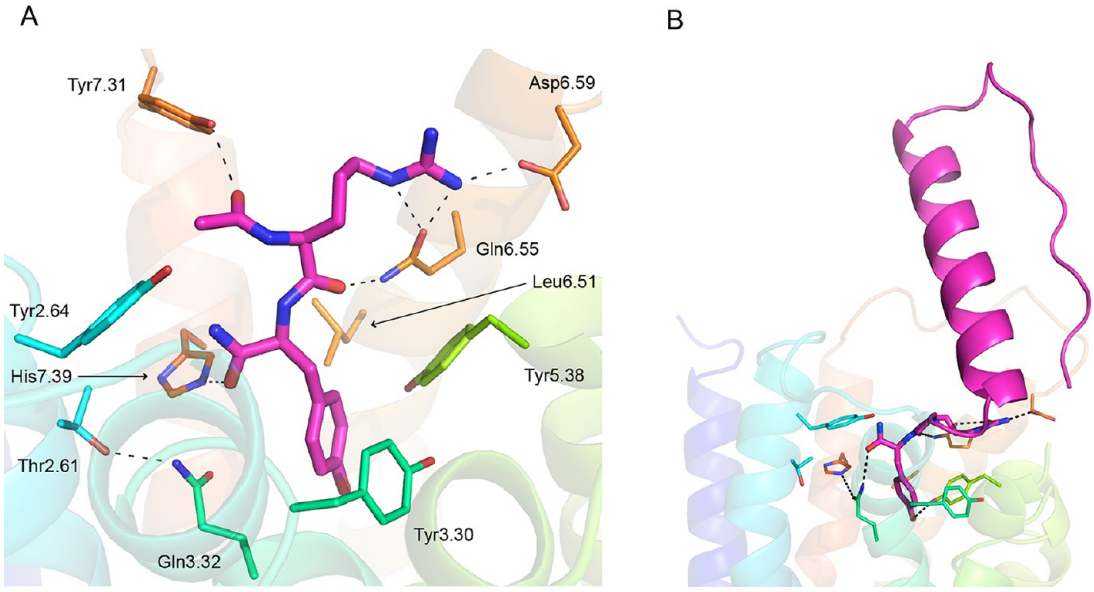

Figure 1. Docking of the C-terminal dipeptide and the full length hNPY to hY2. (A) GOLD docking solution of the acetylated C-terminal dipeptide fragment of hNPY [$CH_3C(O)$-R35-Y36-NH_2, magenta] in the hA_{2A}-based hY2 model. Side chains of the seven hY2 positions investigated by site-directed mutagenesis (Thr2.61, Tyr3.30, Gln3.32, Tyr5.38, Leu6.51, Gln6.55, and His7.39), as well as three previously mutated residues (Tyr2.64, Asp6.59, and Tyr7.31), are shown as sticks. TM helices of the hY2 model are shown in counterclockwise order (TM1, dark blue; TM7, red). (B) Docking solution obtained by HADDOCK for the full hNPY peptide (magenta) in the same hY2 model. The C-terminal dipeptide is explicitly shown as magenta sticks.

transfected without a plasmid to serve as a negative control. The cells were washed twice with PBS and fixed with 4% paraformaldehyde for 10 min. After being washed with PBS, nuclei were stained with 100 μL of DAPI (0.5 μg/mL) at room temperature in the dark for 15 min. The coverslips were rinsed with PBS twice, dried, and mounted upside down on glass slides with mounting medium. Acquired fluorescence was detected with an inverted confocal microscope (Zeiss LSM 510 Meta, Carl Zeiss Inc., Thornwood, NY) and a 63× oil immersion objective (NA = 1.4) and visualized via the accompanying LSM software (Carl Zeiss Inc.).

RESULTS

Selection of Positions for Mutagenesis Based on hY2–Peptide Docking. A computational model of the hY2 receptor and its agonist binding site was developed to guide the selection of the positions to be studied by site-directed mutagenesis. We have recently reported a homology model of hY2, using the hA_{2A} receptor as a template, which was successfully used for the structural interpretation of our site-directed mutagenesis data for positions 2.64, 6.58, and 7.31.[28,29] In this work, we started from this hA_{2A}-based hY2 model to predict the binding mode of the amidated C-terminal region common to all natural agonists of the NPY receptors. This was accomplished in a two-step manner. First, we docked a dipeptide fragment representing the last two C-terminal residues of the ligands with the ligand-based docking protocol GOLD.[35] Thereafter, the information about the binding site, as identified in this ligand docking step, was used to build a series of ambiguous distance restraints to guide the protein–protein docking program HADDOCK[40] in the docking of the full (36 residues) hNPY peptide.

The initial docking results of the $CH_3C(O)$-R35-Y36-NH_2 dipeptide fragment displayed a high level of convergence to one binding mode, which was present in 34 of the 50 generated poses (70%), including the 12 top-scoring poses. This binding mode, shown in Figure 1A, is compatible with the growth of the peptide at the N-terminus of the modeled dipeptide, to represent the full natural agonist in the binding site as will be demonstrated below. Additionally, the amidated C-terminus presents polar interactions with residues Gln3.32 and His7.39 (Figure 1A), a pair of residues completely conserved within the Y receptor family in all jawed vertebrates.[6] The side chain of the tyrosine in the docked dipeptide, representing the peptide-conserved residue Y36, appears to be surrounded by hydrophobic residues, i.e., Tyr3.30, Tyr5.38, and Leu6.51 in hY2. The guanidinium group representing peptide residue R35 forms a salt bridge to Asp6.59, a crucial residue for the binding of agonists to all human Y receptors.[50] This salt bridge was previously hypothesized by the group of Beck-Sickinger for the Y1 receptor but contrasts with their model for the Y2 receptor; they proposed that another peptide arginine, R33, forms a salt bridge to Asp6.59.[31] In addition, we observed a hydrogen bond between R35 and Gln6.55, a residue that when mutated to alanine actually enhances the binding of porcine NPY (pNPY) and hPYY3-36 in the Y2 receptor.[29] Finally, Tyr7.31, mutation of which has been shown to affect agonist binding,[28] is within hydrogen bonding distance of the peptide backbone, in the region where R35 connects to the peptide's preceding residue.

On the basis of these results, residues Tyr3.30, Gln3.32, Tyr5.38, Leu6.51, and Asp6.59, together with Tyr2.64 identified previously,[28] were used to define the binding site, which together with residues R33, R35, and Y36 in the hNPY peptide configured the list of active residues that build up the so-called "ambiguous restraints" in the protein–peptide docking with HADDOCK[40] (see Materials and Methods). Notably, this should be considered as an independent protein–protein docking protocol provided that the ambiguous restraints penalize only the scoring of a given pose if an active residue in one partner does not interact with any of the active or passive residues defined in the other partner; i.e., no pair

dx.doi.org/10.1021/bi400830c | *Biochemistry* 2013, 52, 7987–7998

Table 1. K_d Values of [^{125}I]pPYY and K_i Values of hPYY3-36 and BIIE0246 for WT hY2 and Its Mutants[a]

	[^{125}I]pPYY				hPYY3-36			BIIE0246		
	K_d ± SEM (nM)	B_{max} ± SEM (fmol/mg of protein)	K_d/WT K_d	n	K_i ± SEM (nM)	K_i/WT K_i	n	K_i ± SEM (nM)	K_i/WT K_i	n
WT hY2	0.010 ± 0.001	110 ± 14	1.0	4	0.34 ± 0.11	1.0	5	2.1 ± 0.3	1.0	4
T2.61A	0.093 ± 0.008***	15 ± 2.7	9.3	3	33.7 ± 5.39***	101	3	0.53 ± 0.1*	0.3	3
Q3.32L	nb	–	–	–	–	–	–	–	–	–
Q3.32A	nb	–	–	–	–	–	–	–	–	–
Q3.32E	0.018 ± 0.002	75 ± 8.7	1.8	3	19.0 ± 5.35***	56.9	3	13 ± 2***	6.2	3
Q3.32H	0.028 ± 0.001***	25 ± 4.2	2.8	3	47.0 ± 6.61***	141	3	0.4 ± 0.1**	0.2	3
H7.39L	nb	–	–	–	–	–	–	–	–	–
H7.39A	nb	–	–	–	–	–	–	–	–	–
H7.39Q	0.020 ± 0.002*	64 ± 14	2.0	3	3.09 ± 1.52**	9.2	3	11 ± 2**	5.2	3
Q3.32H +H7.39Q	nb	–	–	–	–	–	–	–	–	–
Y3.30L	0.007 ± 0.001	46 ± 11	0.7	3	0.61 ± 0.1	1.8	3	0.50 ± 0.04**	0.2	5
Y3.30A	0.018 ± 0.004	99 ± 22	1.8	3	1.96 ± 0.48**	5.8	4	1.1 ± 0.03	0.5	3
Y5.38L	0.017 ± 0.002	128 ± 12	1.7	4	3.81 ± 1.30***	11.4	4	0.60 ± 0.1	0.3	3
Y5.38A	0.027 ± 0.005***	222 ± 34	2.7	3	12.7 ± 6.66***	37.4	6	1.4 ± 0.4	0.7	4
L6.51A	0.022 ± 0.003**	52 ± 20	2.2	3	9.69 ± 2.70***	28.9	3	0.9 ± 0.1	0.4	3
Y3.30L +Y5.38L	0.094 ± 0.026***	71 ± 18	9.4	3	12.8 ± 4.01***	38.2	4	2.8 ± 2	1.3	3
Y5.38L +L6.51A	0.038 ± 0.002***	40 ± 2	3.8	3	28.7 ± 15.3***	85.9	3	1.0 ± 0.7	0.5	3
Y3.30L +L6.51A	0.026 ± 0.005**	33 ± 5.5	2.6	3	4.65 ± 0.43***	13.9	3	1.4 ± 1	0.7	3
Q6.55L	nb	–	–	–	–	–	–	–	–	–
Q6.55N	0.021 ± 0.003*	113 ± 2.9	2.1	3	0.310 ± 0.006	1.4	3	16.3 ± 0.82***	7.8	3

[a]The K_d and B_{max} values from the saturation assays and K_i values from competition assays are presented as means ± SEM (nanomolar). K_d/WT K_d and K_i/WT K_i is the x-fold change in affinity compared to that of WT. n is the number of assays performed for each receptor. nb denotes no specific binding. Asterisks indicate the statistical significance of differences in pK_d and pK_i values between WT hY2 and its mutants (*p < 0.05; **p < 0.01; ***p < 0.001). See Figure 3 for graphical display.

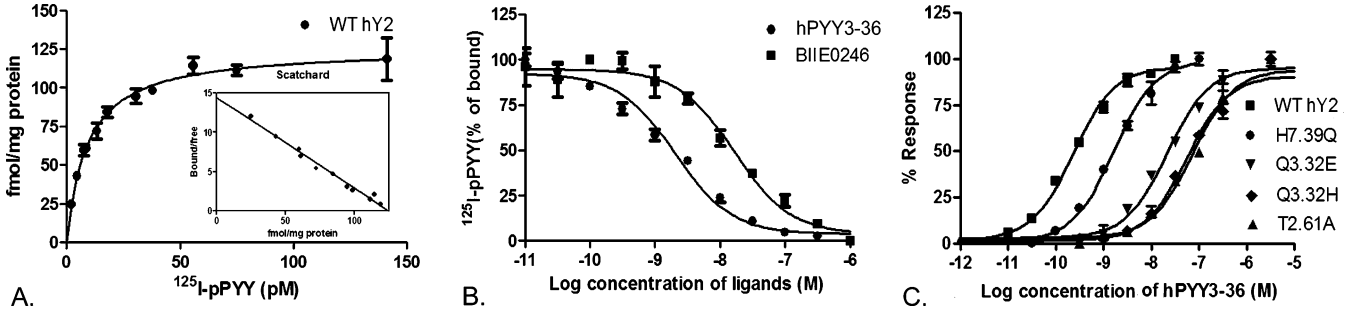

Figure 2. Representative binding curves and dose−response curves for WT hY2 and its mutants. (A) Saturation binding curve of [^{125}I]pPYY for WT hY2. (B) Competition binding curves using hPYY3-36 and BIIE0246 as competing ligands for WT hY2. (C) Dose−response curves that were used to calculate the EC_{50} values of hPYY3-36 for WT hY2 and various hY2 mutants.

distance is imposed at any time. A similar binding orientation for the C-terminal residues of the full peptide is found with this protocol, as one can see in Figure 1B. Despite subtle differences between HADDOCK and GOLD models in the specific hydrogen bond network of the amidated C-terminal residue (Y36), the same residues are involved, mainly Gln3.32 and His7.39. The side chain of this residue appears to be surrounded by the hydrophobic residues described above, and the salt bridge between R35 and Asp6.59 is also maintained in the independent full peptide docking model, together with interactions with Gln6.55. Elongation of the peptide occurs when the α-helix of the peptide (residues 14−32) is placed atop the extracellular side of the TM bundle, forming an angle of ~30° with the TM helices of the receptor and making extensive contacts with EL3. This binding orientation is especially attractive because it is fully compatible with the expected β-sheet folding of the long extracellular loop 2 (EL2), a secondary structure that has been observed in all peptide-binding receptors.[32]

In addition, this hA_{2A}-based hY2 model suggested that the Gln3.32−His7.39 pair could play a pivotal structural role by connecting TM3 and TM7, which is further supported by additional hydrogen bond interaction with Thr2.61 in TM2 (Figure 1A). Thus, the model indicates an important role in either agonist binding or receptor architecture of this residue pair, an observation that is further supported by the total conservation of both Gln3.32 and His7.39 in the NPY family receptors.[6] To test and experimentally validate this modeling hypothesis, and to improve our understanding of the structural

dx.doi.org/10.1021/bi400830c | Biochemistry 2013, 52, 7987−7998

role of these residues, we selected positions Gln3.32, His7.39, and Thr2.61 in hY2 for extensive mutagenesis studies.

Residues Tyr3.30, Tyr5.38, and Leu6.51 were consistently found to bind the side chain of Y36 by both docking protocols, as depicted in Figure 1. Thus, we further selected these positions for mutagenesis. Finally, in light of the proposed interactions with R35 of the peptide, our previous[29] alanine mutant for residue Gln6.55 was complemented here with two mutants: Q6.55L, to see the effect of removing the polarity while retaining the side chain volume, and Q6.55N, which explores the specificity of the polar side chain.

Binding Affinities of [^{125}I]pPYY for WT hY2 and Mutant Receptors. The affinities of the peptide radioligand [^{125}I]pPYY for the WT and mutant hY2 receptors are listed in Table 1, together with the corresponding WT/mutant ratios of K_d values to facilitate quantitative comparison of the effect of a given mutation. A representative saturation curve for [^{125}I]pPYY is shown in Figure 2A. Among the residues forming the hydrogen bond network, a statistically significant decrease in [^{125}I]pPYY affinity was observed for the T2.61A mutant. Milder but nevertheless statistically significant effects were observed when Gln3.32 and His7.39, the other two residues suggested to be involved in the hydrogen bond network, were mutated to polar side chains, namely, Q3.32H and H7.39Q, respectively. The substitution of Gln3.32 with a charged residue, i.e., the Q3.32E mutant, had no significant effect on radioligand binding. Notably, no specific binding of [^{125}I]pPYY was detected for mutants with hydrophobic or small side chains at these two positions (Q3.32L, Q3.32A, H7.39L, and H7.39A) or for the double mutant (Q3.32H+H7.39Q).

For the mutants generated for the three residues forming the proposed binding pocket for Y36 in the peptide, the affinity of the radioligand was significantly decreased for Y5.38A and L6.51A. Cooperative effects (steric requirements) of the three hydrophobic residues on ligand binding were studied by generating three double mutants: Y3.30L+Y5.38L, Y5.38L +L6.51A, and Y3.30L+L6.51A. All three double mutants had significantly reduced radioligand affinities. This additive effect was observed for Y5.38L+L6.51A and Y3.30L+L6.51A compared to the single mutants. No significant change in [^{125}I]pPYY affinity was observed for Y3.30L and Y5.38L mutants, while an ~10-fold decrease in radioligand affinity was observed for the Y3.30L+Y5.38L double mutant.

For residue Gln6.55, it is notable that while the Q6.55N mutation showed a significant 2-fold decrease in [^{125}I]pPYY affinity, no specific radioligand binding was detected for the Q6.55L mutant.

Competition Binding Studies with hPYY3-36 and the Nonpeptide Antagonist BIIE0246. Competition binding of the Y2-selective agonist hPYY3-36 and the nonpeptidergic antagonist BIIE0246 to the WT hY2 and the mutants was evaluated using the radioligand (Table 1). Representative competition curves for hPYY3-36 and BIIE0246 are shown in Figure 2B. A graphical representation of the pK_i values is shown in Figure 3. hPYY3-36 displayed significantly decreased affinity for polar cluster residue mutants: T2.61A, Q3.32E, Q3.32H, and H7.39Q. With regard to the remaining residues suggested to be important by modeling, hPYY3-36 had decreased affinity for mutants Y3.30A, Y5.38A, Y5.38L, and L6.51A, while no change was observed for Y3.30L. All three double mutants were affected more than any of the corresponding single mutants alone, which is in agreement with the results obtained with [^{125}I]pPYY. Overall, the binding of the truncated peptide was more affected by the mutations than the iodinized full peptide (Table 1 and Figure 3).

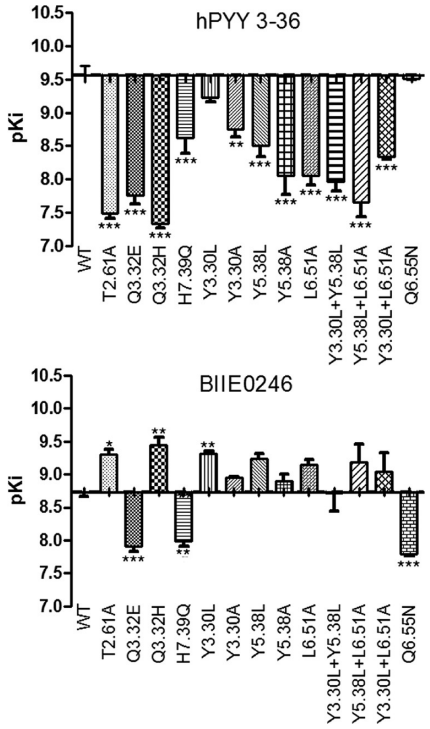

Figure 3. pK_i values of hPYY3-36 and BIIE0246 for WT hY2 and its mutants. The *X* axis intersects the *Y* axis at WT hY2 pK_i values. Bars below the *X* axis indicate decreased affinities and bars above the *X* axis increased affinities. One-way ANOVA with a Dunnett's post test was performed using pK_d and pK_i values for the mutants and WT hY2 (*p < 0.05; **p < 0.01; ***p < 0.001).

The antagonist BIIE0246 had significantly decreased affinity for two mutants involved in the hydrogen bond network, Q3.32E and H7.39Q, although the change was smaller than the change observed with truncated peptide hPYY3-36. In contrast, BIIE0246 showed increased affinity for three mutants: T2.61A and Q3.32H in the hydrogen bond network and Y3.30L. BIIE0246 affinity was more affected by the Q6.55N mutant, as compared with those of agonists [^{125}I]pPYY and hPYY3-36.

Detection of Cellular Expression of WT hY2 and Its Mutants. Membrane expression was confirmed for mutants T2.61A, Q3.32E, Q3.32H, H7.39Q, Q3.32H+H7.39Q, Y3.30L, Y5.38L, Y5.38A, L6.51A, Y3.30L+Y5.38L, Y5.38L+L6.51A, Y3.30L+L6.51A, and Q6.55N (Figure 4). Four of the mutants at residues Gln3.32 and His7.39, namely those with nonpolar amino acid Leu or Ala, as well as the Leu mutation of Q6.55, had no obvious membrane expression. Double mutant Q3.32H +H7.39Q was expressed in only a few cells with low expression level.

Functional Assay of hPYY3-36 for Four Mutants Generated from Residues Forming the Hydrogen Bond Network. The inositol phosphate (IP) functional assay was performed with the agonist hPYY3-36 for mutants T2.61A, Q3.32E, Q3.32H, and H7.39Q. The representative curves are shown in Figure 2C. The potency of hPYY3-36 (expressed as EC_{50}) was significantly decreased for these four mutants compared to that of WT hY2 (Table 2). The decreased potency of hPYY3-36 is consistent with the decrease in its affinity for these mutants.

dx.doi.org/10.1021/bi400830c | *Biochemistry* 2013, 52, 7987−7998

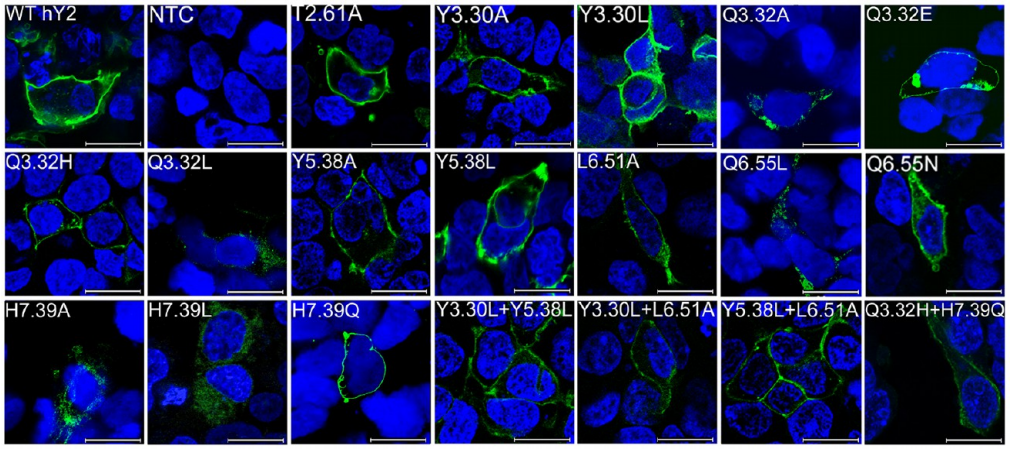

Figure 4. Cellular expression of the WT hY2 and its mutants. Plasmids encoding the hY2 mutants C-terminally fused with green fluorescent protein were transiently transfected into HEK 293 cells to check receptor expression. The scale bar is 20 μm. The nuclei are visualized with DAPI (blue). WT hY2, negative control, T2.61A, Y3.30A, Y3.30L, Q3.32A, Q3.32E, Q3.32H, Q3.32L, Y5.38A, Y5.38L, L6.51A, Q6.55L, Q6.55N, H7.39Q, H7.39L, H7.39A, Y3.30L+L6.51A, Y3.30L+Y5.38L, Y5.38L+L6.51A, and Q3.32H+H7.39Q.

Table 2. EC_{50} Values of hPYY3-36 in the Inositol Phosphate Assay for WT hY2 and Mutants Generated from Residues Forming the Hydrogen Bond Network[a]

	EC_{50} ± SEM (nM)	EC_{50}/WT EC_{50}	K_i ± SEM (nM)	K_i/WT K_i
WT hY2	0.311 ± 0.038	1	0.34 ± 0.11	1.0
T2.61A	71.3 ± 21.3***	229	33.7 ± 5.39***	100
Q3.32E	14.1 ± 5.0***	45.2	19.0 ± 5.35***	56.9
Q3.32H	64.6 ± 16.5***	208	47.0 ± 6.61***	141
H7.39Q	1.63 ± 0.38**	5.25	3.09 ± 1.52**	9.2

[a]The EC_{50} values are presented as means ± SEM (nanomolar). EC_{50}/WT EC_{50} is the *x*-fold change in potency compared to that of WT hY2. Three independent assays were performed in triplicate for each mutant. Asterisks show the statistical significance of differences in pEC_{50} values between WT hY2 and its mutants (*$p < 0.05$; **$p < 0.01$; ***$p < 0.001$).

Structural Evaluation of Binding Data Using an Active-like hY2 Homology Model, Docking, and Molecular Dynamics Simulations. The recent determination of the rat NTSR1 structure, released during the course of this project, provided us with the first crystal structure of a peptide-binding GPCR with an agonist bound. Even though this does not necessarily mean that the receptor is in a fully active conformation (i.e., no intracellular G-protein is present in the crystal structure), the presence of the agonist and comparison with other active GPCRs can guarantee that the template is in an active-like conformation.[45] Importantly, NTSR1 is also a member of the β-branch of class A GPCRs, like the NPY receptor family, according to the phylogenetic tree derived by Fredriksson et al.,[51] although the level of sequence identity between hY2 and rNTSR1 is a rather modest 18% overall and 26% in the transmembrane helices. We decided to create a new model on the basis of this template to compare with the model that we used as a guide for the selection of positions for mutagenesis and to offer a complementary interpretation of the results. The TM helices tilt slightly differently, in particular TM6, in agreement with the observed differences between the two templates and the activation-related conformational changes in GPCRs.[52−54] However, the same amino acids line the cavity walls, with the notable exception of residue Tyr3.30, which in the new model is oriented toward the membrane.

The explicit consideration of all loop regions in this active-like model of hY2 encouraged us to directly investigate the binding mode of the C-terminal pentapeptide (^{32}TRQRY^{36}-amide), representing the common fragment to the NPY/PYY peptides, by means of a more advance computational protocol: an automated, induced-fit peptide docking was followed by molecular dynamics simulations with explicit consideration of the solvent and membrane. The receptor−ligand structure, depicted in Figure 5, shows a somewhat different interaction pattern compared to that of our initial, A_{2A}-based model, but the same residues are involved. The side chain of Y36 is positioned in a deep pocket situated among TM3, TM6, and TM7, showing contacts with hY2 residues Q3.32, V3.36, L6.51, Q6.55, and H7.39, in addition to a water-mediated hydrogen bond with the backbone of TM7. The C-terminal amide of the peptide forms hydrogen bonds with Y5.38, S5.42, and Q6.55, and it is the side chain of Q34 in this binding orientation that forms a hydrogen bond to the conserved Q3.32 in the receptor. The electrostatic interaction network defined by the positively charged residues of the peptide, R33 and R35, is intricate. Both residues form salt bridges with D6.59 in TM6 and E5.24 located in EL2, reinforced by hydrogen bonds of R33 with T5.23 and V6.58 (backbone) and of R35 with S5.39. The peptide backbone is further stabilized with hydrogen bonds to water molecules from the bulk solvent, as well as with hY2 residues Q6.55 and Y7.31. Finally, the position of T32 is compatible with the extension of the peptide to represent the full NPY or PYY agonists in the binding site. The fact that we have explicitly considered a modeled conformation of EL2 precluded us from attempting an automated protein−protein docking with HADDOCK, because the conformational flexibility that one needs to explore the backbone of this long loop is beyond the limitations allowed with this program.

dx.doi.org/10.1021/bi400830c | *Biochemistry* 2013, 52, 7987−7998

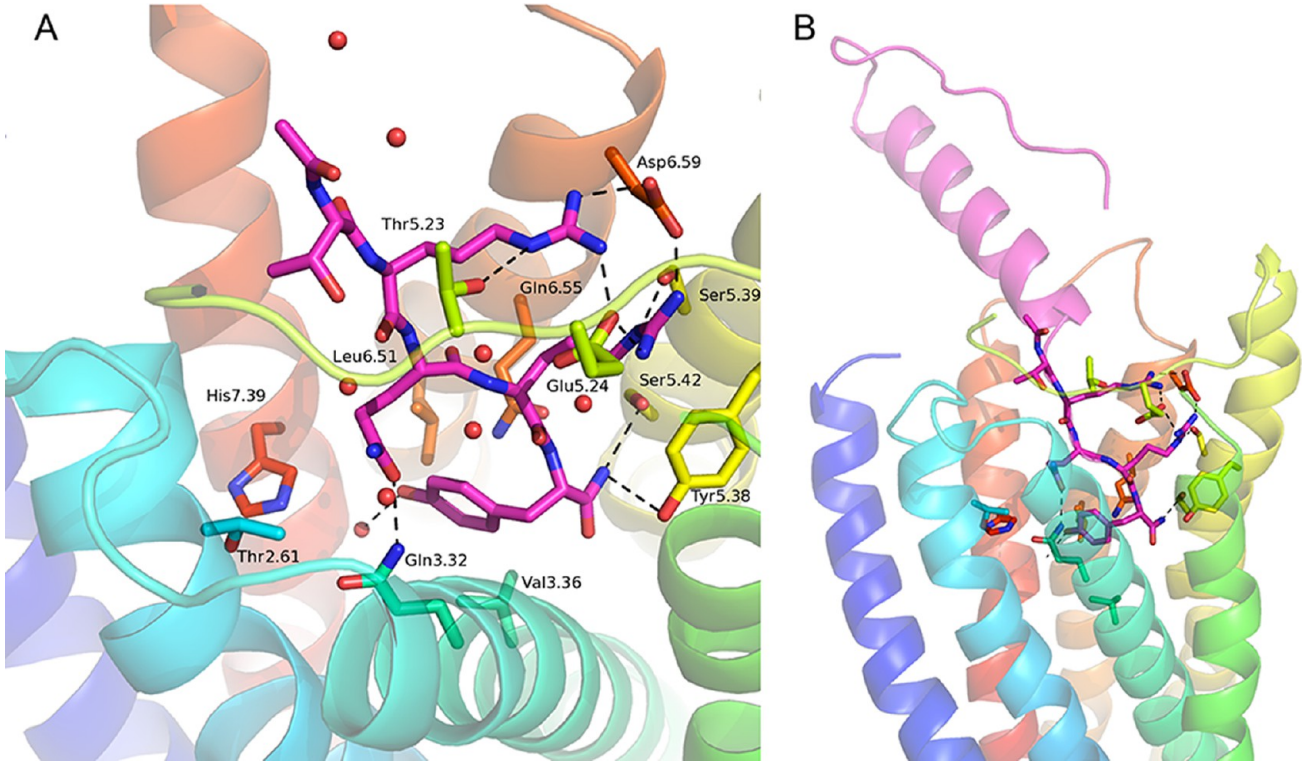

Figure 5. Active-like (NTSR1-based) hY2 receptor model. (A) Docking solution of the C-terminal pentapeptide of the NPY/PYY family of peptides. Side chains of the hY2 positions discussed in the text are shown as sticks, and water molecules in contact with the ligand are shown as spheres. (B) Manual docking of the full hNPY peptide (magenta) with the C-terminal pentapeptide fragment depicted as sticks.

Instead, a manual docking of the NPY crystal structure, using the pose of the ^{32}TRQRY^{36}-NH$_2$ fragment discussed above as an attachment point, was performed to obtain clues about whether the binding mode proposed for the pentapeptide would be compatible with a binding orientation of the full peptide. The result is shown in Figure 5B, where it can be observed that the α-helix of the peptide would lie on the cavity between EL2 and EL3, with an ~30° inclination with respect to the membrane plane, in a similar way as suggested by the preliminary docking protocol using the initial A_{2A}-based model as shown in Figure 1B.

DISCUSSION

Our initial modeling identified a group of polar and highly conserved amino acid residues in the NPY receptor family (Thr2.61, Gln3.32, and His7.39), which appear to be oriented toward the binding cavity. These three residues create a hydrogen bond network with a proposed double role. First, they may be important for receptor packing by mediating a helix−helix interaction between TM3 and TM7; second, they support the binding of the invariant C-terminal part of the native peptidic agonists, according to our ligand binding hypothesis (see Figures 1 and 5A). Furthermore, the orientation of the side chains of Gln3.32 and His7.39 in hY2 resembles the roles of conserved residues Asp3.32 and Asn7.39 in the crystal structures of adrenergic receptors,[55,56] where this pair is crucial for the binding of the charged amino group of both agonists and antagonists. More recently, the crystal structure of NTSR1 has shown that the residues in the corresponding positions of this triad, namely, Arg3.32, Asn7.39, and Glu2.61, are conserved in the NTSRs and form a polar network.[45]

Gln3.32 in hY2 was first mutated to a glutamic acid (Q3.32E), to evaluate the impact of charge redistribution without changing the shape and flexibility of the original side chain. In this scenario, His7.39 is likely to be protonated to counterbalance the new negative charge and maintain a neutral net charge of the microenvironment. Such charge redistribution at positions 3.32 and 7.39 is predicted to have an unfavorable effect on receptor−ligand interactions, as suggested by its impact on both agonist and antagonist binding. This specificity of the residue at position 3.32 was supported by the even lower affinity of the peptide agonists for the histidine mutant (Q3.32H), suggesting a specific role of the Gln3.32 side chain in the binding of the C-terminal tail of the peptide agonists. In this line of thinking, the H7.39Q conservative mutation was designed to preserve the polarity while removing the aromaticity of the WT histidine, which produced a significantly decreased affinity for both peptide agonists and BIIE0246, thus leading to the conclusion that this position plays a role in the interaction with both types of ligands. Our results are in agreement with previous site-directed mutagenesis of the corresponding conserved positions in hY1, where mutations of Gln3.32 resulted in major effects on agonist binding or even receptor expression,[22,26] while a H7.39G mutant on the same receptor led to a decreased PYY affinity.[22]

The possibility of a structural role of these two polar residues that could indirectly affect ligand binding was investigated by constructing the reciprocal mutant Q3.32H+H7.39Q. This double mutation led to completely undetectable radioligand binding and a poor cellular expression level that is in agreement with the idea of a direct interaction between the two residues. The poor receptor expression for this reciprocal double mutant implies that the exact geometry of this polar network is very

dx.doi.org/10.1021/bi400830c | *Biochemistry* 2013, 52, 7987−7998

sensitive to the particular location and rotameric nature of the residues implied, which agrees with our structural model in which Thr2.61 is also involved. Further, a total lack of polarity at either position Gln3.32 or His7.39, explored by substitutions to leucine (preserving the side chain shape) and further to alanine (to remove most of the side chain atoms), also compromises the cell membrane expression of the receptor (see Figure 4). The role of Thr2.61 in receptor−agonist interactions was confirmed with the corresponding alanine mutant (T2.61A), which showed a significant decrease in agonist affinity. This could be perfectly explained by an indirect effect, i.e., that Thr2.61 maintains the proper conformation of residue Gln3.32 and/or His7.39 through polar interactions. Conversely, the affinity of the antagonist BIIE0246 was increased, an effect similar to that observed for one of the mutants at position 3.32 (Q3.32H). These results indicate a different pattern of interactions with these residues as compared to that of the agonists. We conclude that conserved residues Thr2.61, Gln3.32, and His 7.39 are important for peptide binding in addition to their structural role, in agreement with our two independently derived computational models shown in Figures 1 and 5A. The conservation of these three residues among NPY family receptors suggests that they may have similar functions in all of the NPY receptor subtypes, and possibly even in related peptide-binding receptors such as the orexin receptors.[57]

In our initial modeling based on the A_{2A} template (Figure 1A), a binding pocket formed by Tyr3.30, Tyr5.38, and Leu6.51 is the binding site of the side chain of Y36 in the peptide. This hypothesis was evaluated by single or double mutations to alanine or leucine at each of these positions. However, Tyr3.30 was found to have a minor role in peptide binding, which is indeed in agreement with the revised, active-like model of hY2 (Figure 5A) in which this residue does not face the binding cavity, and only a minor role in protein stability would be expected. Single mutations at Tyr5.38 and Leu6.51 as hypothesized reduced the level of agonist binding, and this effect was greater in the double mutant Y5.38L+L6.51A. This result supports the role of residues Tyr5.38 and Leu6.51 in the binding of position Y36 of the peptide agonists, as consistently observed in the active-like model (Figure 5A). In contrast, the binding of the antagonist BIIE0246 was not affected by any of the single or double mutations in this pocket, indicating that this region is not contacted by this antagonist. The effect of mutating the corresponding Tyr5.38 and Leu6.51 residues in hY1 has been previously reported: a change of Tyr5.38 to Ala affected antagonist binding in two different studies,[22,24] while Leu6.51, a residue conserved among all human NPY receptors, is also involved in the binding of the agonist PYY to the Y1 receptor.[23] Taken together, the results from previous studies of Y1 and our current results for the Y2 receptor strongly suggest that positions 5.38 and 6.51 should be a conserved peptide-binding region between hY1 and hY2 receptors.

A polar side chain at position 6.55 has been shown to be important for ligand binding[34] or selectivity[58] in several GPCR families. In the NPY family, there is always a polar side chain in this position, yet it differs between receptor subtypes: Asn in Y1 and Y4, Gln in Y2, and His in Y5. In a recent study,[29] we reported enhanced binding of pNPY to the hY2 mutant Q6.55A. However, in light of our initial modeling of peptide binding, Gln6.55 could make extensive hydrogen bonds with R35 in the peptide (see Figure 1). Therefore, we mutated Gln6.55 to Leu to avoid side chain polarity while maintaining shape and to Asn that occupies the corresponding position in Y1 and Y4. The agonist radioligand displayed a small but statistically significant decrease in affinity for the Q6.55N mutant, pointing to a role of this position in the subtype-specific peptide−receptor interactions. The affinity of BIIE0246 for Q6.55N decreased somewhat more, suggesting an attachment point for this antagonist. The fact that the Q6.55L mutant lost membrane expression could indicate that a hydrophobic side chain at this position disrupts the proper packing of the receptor's TM regions. These results necessitate a reinterpretation of the previously reported enhanced binding effect of replacement with alanine;[29] its short side chain may interact with a water molecule that might restore the hydrogen bond network.

The crystal structure of NTSR1, reported during the course of this work, provided us with an agonist-bound template belonging to the same branch (β-branch of class A GPCRs) as the NPY receptors. The hY2−^{32}TRQRY^{36}-amide complex generated on the basis of this template is shown in Figure 5. The complex is in good agreement with the mutagenesis data presented here as well as previously,[28−31,50,59] and the stability of this binding pose has been confirmed by MD simulations. Further, this binding mode of the ^{32}TRQRY^{36}-amide is compatible with a manually obtained docking hypothesis of the full NPY peptide as shown in Figure 5B, although with the experimental data at hand the binding mode of the N-terminal part of the peptide remains uncertain. Preliminary docking of the antagonist BIIE0246 resulted in several possible docking poses (not shown) and will require a mutagenesis approach different from the one used here for the native peptide agonists.

According to a classical alanine scan study of hNPY, the main decreases in affinity were observed by mutations in the conserved C-terminal pentapeptide (^{32}TRQRY^{36}-amide).[50] This is explained well by our model, in which this part of the agonist interacts with the orthosteric binding site of the hY2 receptor, i.e., residues Q3.32, L6.51, D6.59, and H7.39. These residues are well-conserved in NPY receptors but rather unusual in the corresponding positions of other GPCRs.[60]

Further, positions R33 and R35 and the C-terminal amide of the peptide make extensive interactions with a number of polar side chains located in EL2 or the extracellular tips of TM5 and TM6 (Figure 5A). All these residues either are conserved within a receptor family or are receptor subtype-specific and have been found to be often involved in GPCR−ligand binding.[61,62] Specifically, the double salt bridge of each arginine in the peptide with both E5.24 and D6.59 agrees well with published functional assay data for complementary mutations in these acidic residues.[31] We provide in Figure 6 a new analysis of these data in light of the results presented here, where the free energy of binding that was lost upon each mutation is approximated using Coulomb's law. The numbers are qualitatively in good agreement with the experimental EC_{50} values reported by Merten et al.,[31] providing further support for the interaction pattern in Figure 6. It should be noted, though, that the quantitative loss of signal transduction (EC_{50} values) cannot be directly translated to binding affinity or binding free energy values, because there might be other factors distinct from binding affinity that affect the measured ligand efficacy. One should also stress here that a single mutation of any of the key ionic residues depicted in Figure 6 will probably alter the local interaction pattern of the ionic network or could even influence the overall peptide binding mode. Such indirect effects produced by a single (or double) mutation cannot be

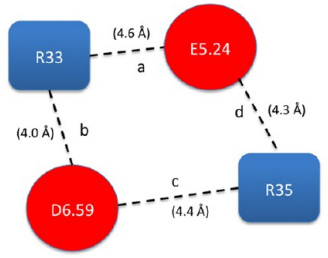

hY2R mutations	hNPY mutations: WT		R33A		R35A	
	EC_{50}/WT EC_{50} (ref 31)		$\Delta\Delta G_{bind}$ WT-mutant (kcal/mol) * (remaining ion pairs, see schema)			
WT	1	0.0	>309	1.9[b,c]	203	1.9[a,b]
D6.59A	>619	2.0[a,d]	>485	2.9[d]	>1000**	2.9[a]
E5.24A	51	1.9[b,c]	>1000	2.9[c]	>1000	2.8[b]

* Estimated from Coulombs law: $\Delta G=(332/\varepsilon_o \cdot r) \cdot \{qi \cdot qj\}$, with $\varepsilon_o=80$
** Not determined with sufficient accuracy as in Ref 31

Figure 6. Structure–activity relationship for the mutations affecting peptide–receptor ion pairs. The schematic representation of the ion pairs is derived from the structural model presented in Figure 5. The mutagenesis data from ref 31 are correlated in the table with the estimation of binding free energy lost upon each mutation, using Coulomb's law with a high dielectric constant and the average distances between ion pairs, as indicated in parentheses.

considered in any structure–activity relationships drawn from the functional assay data of these mutants.

Altogether, our iterative combination of computational modeling, site-directed mutagenesis, and binding studies adds important information to elucidate the binding mode of agonists to the hY2 receptor and is currently used to guide further experiments in our lab to establish structure–activity relationships for native agonists and interactions with non-peptidergic antagonists of the NPY family receptors.

AUTHOR INFORMATION

Corresponding Author

*Telephone: +46184714173. Fax: +46-18 511 540. E-mail: dan.larhammar@neuro.uu.se.

Author Contributions

B.X., H.F., L.B., H.G.-d.-T., I.L., J.Å., and D.L. participated in research design. B.X., H.F., L.B., J.P., H.G.-d.-T., and I.L. conducted experiments. B.X., H.F., L.B., J.P., H.G.-d.-T., I.L., and N.M. performed data analysis. All authors wrote or contributed to the writing of the manuscript.

Funding

This work was supported by grants from the Swedish Research Council (2011-2438 and 2009-4865) and by the Swedish strategic research program eSSENCE. H.G.-d.-T. acknowledges financial support from the National Spanish Research program (SAF2001-30104) as well as a research stay in Uppsala University from Xunta de Galicia.

Notes

The authors declare no competing financial interest.

ACKNOWLEDGMENTS

We thank Md Rashidur Rahman and Björn Edlund for help with the experiments.

ABBREVIATIONS

NPY, neuropeptide Y; PYY, peptide YY; hYx and pYx, human and porcine neuropeptide Y receptor type x, respectively; GPCR, G-protein-coupled receptor; WT, wild type; rNTSR1, rat neurotensin receptor type 1; TM, transmembrane region; MD, molecular dynamics; PBC, periodic boundary conditions; IP, inositol phosphates; hA_{2A}, human adenosine A_{2A} receptor; SEM, standard error of the mean.

REFERENCES

(1) Zhang, L., Bijker, M. S., and Herzog, H. (2011) The neuropeptide Y system: Pathophysiological and therapeutic implications in obesity and cancer. *Pharmacol. Ther. 131*, 91–113.

(2) Brothers, S. P., and Wahlestedt, C. (2010) Therapeutic potential of neuropeptide Y (NPY) receptor ligands. *EMBO Mol. Med. 2*, 429–439.

(3) Chugh, P. K., and Sharma, S. (2012) Recent advances in the pathophysiology and pharmacological treatment of obesity. *J. Clin. Pharm. Ther. 37*, 525–535.

(4) Sundström, G., Larsson, T. A., Brenner, S., Venkatesh, B., and Larhammar, D. (2008) Evolution of the neuropeptide Y family: New genes by chromosome duplications in early vertebrates and in teleost fishes. *Gen. Comp. Endrocrinol. 155*, 705–716.

(5) Larhammar, D., Wraith, A., Berglund, M. M., Holmberg, S. K., and Lundell, I. (2001) Origins of the many NPY-family receptors in mammals. *Peptides 22*, 295–307.

(6) Larsson, T. A., Tay, B. H., Sundström, G., Fredriksson, R., Brenner, S., Larhammar, D., and Venkatesh, B. (2009) Neuropeptide Y-family peptides and receptors in the elephant shark, *Callorhinchus milii*, confirm gene duplications before the gnathostome radiation. *Genomics 93*, 254–260.

(7) Larsson, T. A., Olsson, F., Sundström, G., Lundin, L. G., Brenner, S., Venkatesh, B., and Larhammar, D. (2008) Early vertebrate chromosome duplications and the evolution of the neuropeptide Y receptor gene regions. *BMC Evol. Biol. 8*, 184.

(8) Sundström, G., Xu, B., Larsson, T. A., Heldin, J., Bergqvist, C. A., Fredriksson, R., Conlon, J. M., Lundell, I., Denver, R. J., and Larhammar, D. (2012) Characterization of the neuropeptide Y system in the frog *Silurana tropicalis* (Pipidae): Three peptides and six receptor subtypes. *Gen. Comp. Endrocrinol. 177*, 322–331.

(9) Matsumoto, M., Nomura, T., Momose, K., Ikeda, Y., Kondou, Y., Akiho, H., Togami, J., Kimura, Y., Okada, M., and Yamaguchi, T. (1996) Inactivation of a novel neuropeptide Y/peptide YY receptor gene in primate species. *J. Biol. Chem. 271*, 27217–27220.

(10) Michel, M. C., Beck-Sickinger, A., Cox, H., Doods, H. N., Herzog, H., Larhammar, D., Quirion, R., Schwartz, T., and Westfall, T. (1998) XVI. International Union of Pharmacology recommendations for the nomenclature of neuropeptide Y, peptide YY, and pancreatic polypeptide receptors. *Pharmacol. Rev. 50*, 143–150.

(11) Bard, J. A., Walker, M. W., Branchek, T. A., and Weinshank, R. L. (1995) Cloning and functional expression of a human Y4 subtype receptor for pancreatic polypeptide, neuropeptide Y, and peptide YY. *J. Biol. Chem. 270*, 26762–26765.

(12) Berglund, M. M., Lundell, I., Eriksson, H., Soll, R., Beck-Sickinger, A. G., and Larhammar, D. (2001) Studies of the human, rat, and guinea pig Y4 receptors using neuropeptide Y analogues and two distinct radioligands. *Peptides 22*, 351–356.

(13) Gehlert, D. R., Schober, D. A., Beavers, L., Gadski, R., Hoffman, J. A., Smiley, D. L., Chance, R. E., Lundell, I., and Larhammar, D. (1996) Characterization of the peptide binding requirements for the cloned human pancreatic polypeptide-preferring receptor. *Mol. Pharmacol. 50*, 112–118.

(14) Lundell, I., Blomqvist, A. G., Berglund, M. M., Schober, D. A., Johnson, D., Statnick, M. A., Gadski, R. A., Gehlert, D. R., and Larhammar, D. (1995) Cloning of a human receptor of the NPY receptor family with high affinity for pancreatic polypeptide and peptide YY. *J. Biol. Chem. 270*, 29123–29128.

(15) Cabrele, C., and Beck-Sickinger, A. G. (2000) Molecular characterization of the ligand-receptor interaction of the neuropeptide Y family. *J. Pept. Sci. 6*, 97−122.
(16) Yulyaningsih, E., Zhang, L., Herzog, H., and Sainsbury, A. (2011) NPY receptors as potential targets for anti-obesity drug development. *Br. J. Pharmacol. 163*, 1170−1202.
(17) Doods, H., Gaida, W., Wieland, H. A., Dollinger, H., Schnorrenberg, G., Esser, F., Engel, W., Eberlein, W., and Rudolf, K. (1999) BIIE0246: A selective and high affinity neuropeptide Y Y(2) receptor antagonist. *Eur. J. Pharmacol. 384*, R3−R5.
(18) Bonaventure, P., Nepomuceno, D., Mazur, C., Lord, B., Rudolph, D. A., Jablonowski, J. A., Carruthers, N. I., and Lovenberg, T. W. (2004) Characterization of N-(1-Acetyl-2,3-dihydro-1H-indol-6-yl)-3-(3-cyano-phenyl)-N-[1-(2-cyclopen tyl-ethyl)-piperidin-4yl]-acrylamide (JNJ-5207787), a small molecule antagonist of the neuropeptide Y Y2 receptor. *J. Pharmacol. Exp. Ther. 308*, 1130−1137.
(19) Shoblock, J. R., Welty, N., Nepomuceno, D., Lord, B., Aluisio, L., Fraser, I., Motley, S. T., Sutton, S. W., Morton, K., Galici, R., Atack, J. R., Dvorak, L., Swanson, D. M., Carruthers, N. I., Dvorak, C., Lovenberg, T. W., and Bonaventure, P. (2010) In vitro and in vivo characterization of JNJ-31020028 (N-(4-{4-[2-(diethylamino)-2-oxo-1-phenylethyl]piperazin-1-yl}-3-fluorophenyl)-2-pyridin-3-ylbenzamide), a selective brain penetrant small molecule antagonist of the neuropeptide Y Y(2) receptor. *Psychopharmacology 208*, 265−277.
(20) Brothers, S. P., Saldanha, S. A., Spicer, T. P., Cameron, M., Mercer, B. A., Chase, P., McDonald, P., Wahlestedt, C., and Hodder, P. S. (2010) Selective and brain penetrant neuropeptide Y Y2 receptor antagonists discovered by whole-cell high-throughput screening. *Mol. Pharmacol. 77*, 46−57.
(21) Cerda-Reverter, J. M., and Larhammar, D. (2000) Neuropeptide Y family of peptides: Structure, anatomical expression, function, and molecular evolution. *Biochem. Cell Biol. 78*, 371−392.
(22) Du, P., Salon, J. A., Tamm, J. A., Hou, C., Cui, W., Walker, M. W., Adham, N., Dhanoa, D. S., Islam, I., Vaysse, P. J., Dowling, B., Shifman, Y., Boyle, N., Rueger, H., Schmidlin, T., Yamaguchi, Y., Branchek, T. A., Weinshank, R. L., and Gluchowski, C. (1997) Modeling the G-protein-coupled neuropeptide Y Y1 receptor agonist and antagonist binding sites. *Protein Eng. 10*, 109−117.
(23) Kanno, T., Kanatani, A., Keen, S. L., Arai-Otsuki, S., Haga, Y., Iwama, T., Ishihara, A., Sakuraba, A., Iwaasa, H., Hirose, M., Morishima, H., Fukami, T., and Ihara, M. (2001) Different binding sites for the neuropeptide Y Y1 antagonists 1229U91 and J-104870 on human Y1 receptors. *Peptides 22*, 405−413.
(24) Sautel, M., Rudolf, K., Wittneben, H., Herzog, H., Martinez, R., Munoz, M., Eberlein, W., Engel, W., Walker, P., and Beck-Sickinger, A. G. (1996) Neuropeptide Y and the nonpeptide antagonist BIBP 3226 share an overlapping binding site at the human Y1 receptor. *Mol. Pharmacol. 50*, 285−292.
(25) Sautel, M., Martinez, R., Munoz, M., Peitsch, M. C., Beck-Sickinger, A. G., and Walker, P. (1995) Role of a hydrophobic pocket of the human Y1 neuropeptide Y receptor in ligand binding. *Mol. Cell. Endocrinol. 112*, 215−222.
(26) Sjodin, P., Holmberg, S. K., Åkerberg, H., Berglund, M. M., Mohell, N., and Larhammar, D. (2006) Re-evaluation of receptor-ligand interactions of the human neuropeptide Y receptor Y1: A site-directed mutagenesis study. *Biochem. J. 393*, 161−169.
(27) Walker, P., Munoz, M., Martinez, R., and Peitsch, M. C. (1994) Acidic residues in extracellular loops of the human Y1 neuropeptide Y receptor are essential for ligand binding. *J. Biol. Chem. 269*, 2863−2869.
(28) Åkerberg, H., Fällmar, H., Sjodin, P., Boukharta, L., Gutiérrez-de-Terán, H., Lundell, I., Mohell, N., and Larhammar, D. (2010) Mutagenesis of human neuropeptide Y/peptide YY receptor Y2 reveals additional differences to Y1 in interactions with highly conserved ligand positions. *Regul. Pept. 163*, 120−129.
(29) Fällmar, H., Åkerberg, H., Gutiérrez-de-Terán, H., Lundell, I., Mohell, N., and Larhammar, D. (2011) Identification of positions in the human neuropeptide Y/peptide YY receptor Y2 that contribute to pharmacological differences between receptor subtypes. *Neuropeptides 45*, 293−300.
(30) Berglund, M. M., Fredriksson, R., Salaneck, E., and Larhammar, D. (2002) Reciprocal mutations of neuropeptide Y receptor Y2 in human and chicken identify amino acids important for antagonist binding. *FEBS Lett. 518*, 5−9.
(31) Merten, N., Lindner, D., Rabe, N., Rompler, H., Morl, K., Schoneberg, T., and Beck-Sickinger, A. G. (2007) Receptor subtype-specific docking of Asp6.59 with C-terminal arginine residues in Y receptor ligands. *J. Biol. Chem. 282*, 7543−7551.
(32) Katritch, V., Cherezov, V., and Stevens, R. C. (2013) Structure-function of the G protein-coupled receptor superfamily. *Annu. Rev. Pharmacol. Toxicol. 53*, 531−556.
(33) Ballesteros, J., and Palczewski, K. (2001) G protein-coupled receptor drug discovery: Implications from the crystal structure of rhodopsin. *Curr. Opin. Drug Discovery Dev. 4*, 561−574.
(34) Jaakola, V. P., Griffith, M. T., Hanson, M. A., Cherezov, V., Chien, E. Y., Lane, J. R., Ijzerman, A. P., and Stevens, R. C. (2008) The 2.6 angstrom crystal structure of a human A2A adenosine receptor bound to an antagonist. *Science 322*, 1211−1217.
(35) Jones, G., Willett, P., Glen, R. C., Leach, A. R., and Taylor, R. (1997) Development and validation of a genetic algorithm for flexible docking. *J. Mol. Biol. 267*, 727−748.
(36) Verdonk, M. L., Cole, J. C., Hartshorn, M. J., Murray, C. W., and Taylor, R. D. (2003) Improved protein-ligand docking using GOLD. *Proteins 52*, 609−623.
(37) Glover, I., Haneef, I., Pitts, J., Wood, S., Moss, D., Tickle, I., and Blundell, T. (1983) Conformational flexibility in a small globular hormone: X-ray analysis of avian pancreatic polypeptide at 0.98-Å resolution. *Biopolymers 22*, 293−304.
(38) Sali, A., and Blundell, T. L. (1993) Comparative protein modelling by satisfaction of spatial restraints. *J. Mol. Biol. 234*, 779−815.
(39) Shen, M. Y., and Sali, A. (2006) Statistical potential for assessment and prediction of protein structures. *Protein Sci. 15*, 2507−2524.
(40) Dominguez, C., Boelens, R., and Bonvin, A. M. J. J. (2003) HADDOCK: A protein-protein docking approach based on biochemical or biophysical information. *J. Am. Chem. Soc. 125*, 1731−1737.
(41) de Vries, S. J., van Dijk, A. D., Krzeminski, M., van Dijk, M., Thureau, A., Hsu, V., Wassenaar, T., and Bonvin, A. M. (2007) HADDOCK versus HADDOCK: New features and performance of HADDOCK2.0 on the CAPRI targets. *Proteins 69*, 726−733.
(42) Hubbard, S. J., and Thornton, J. M. (1993) *NACCESS*, Department of Biochemistry and Molecular Biology, University College London, London.
(43) Kersey, P. J., Staines, D. M., Lawson, D., Kulesha, E., Derwent, P., Humphrey, J. C., Hughes, D. S., Keenan, S., Kerhornou, A., Koscielny, G., Langridge, N., McDowall, M. D., Megy, K., Maheswari, U., Nuhn, M., Paulini, M., Pedro, H., Toneva, I., Wilson, D., Yates, A., and Birney, E. (2012) Ensembl Genomes: An integrative resource for genome-scale data from non-vertebrate species. *Nucleic Acids Res. 40*, D91−D97.
(44) Waterhouse, A. M., Procter, J. B., Martin, D. M., Clamp, M., and Barton, G. J. (2009) Jalview Version 2: A multiple sequence alignment editor and analysis workbench. *Bioinformatics 25*, 1189−1191.
(45) White, J. F., Noinaj, N., Shibata, Y., Love, J., Kloss, B., Xu, F., Gvozdenovic-Jeremic, J., Shah, P., Shiloach, J., Tate, C. G., and Grisshammer, R. (2012) Structure of the agonist-bound neurotensin receptor. *Nature 490*, 508−513.
(46) Sherman, W., Day, T., Jacobson, M. P., Friesner, R. A., and Farid, R. (2006) Novel procedure for modeling ligand/receptor induced fit effects. *J. Med. Chem. 49*, 534−553.
(47) Gutierrez-de-Teran, H., Bello, X., and Rodriguez, D. (2013) Characterization of the dynamic events of GPCRs by automated computational simulations. *Biochem. Soc. Trans. 41*, 205−212.

(48) Kostenis, E. (2002) Potentiation of GPCR-signaling via membrane targeting of G protein α subunits. *J. Recept. Signal Transduction Res. 22*, 267−281.
(49) Johansson, L., Ekholm, M. E., and Kukkonen, J. P. (2007) Regulation of OX1 orexin/hypocretin receptor-coupling to phospholipase C by Ca^{2+} influx. *Br. J. Pharmacol. 150*, 97−104.
(50) Beck-Sickinger, A. G., Wieland, H. A., Wittneben, H., Willim, K. D., Rudolf, K., and Jung, G. (1994) Complete L-alanine scan of neuropeptide Y reveals ligands binding to Y1 and Y2 receptors with distinguished conformations. *Eur. J. Biochem. 225*, 947−958.
(51) Fredriksson, R., Lagerstrom, M. C., Lundin, L. G., and Schioth, H. B. (2003) The G-protein-coupled receptors in the human genome form five main families. Phylogenetic analysis, paralogon groups, and fingerprints. *Mol. Pharmacol. 63*, 1256−1272.
(52) Rasmussen, S. G., Choi, H. J., Fung, J. J., Pardon, E., Casarosa, P., Chae, P. S., Devree, B. T., Rosenbaum, D. M., Thian, F. S., Kobilka, T. S., Schnapp, A., Konetzki, I., Sunahara, R. K., Gellman, S. H., Pautsch, A., Steyaert, J., Weis, W. I., and Kobilka, B. K. (2011) Structure of a nanobody-stabilized active state of the β2 adrenoceptor. *Nature 469*, 175−180.
(53) Xu, F., Wu, H., Katritch, V., Han, G. W., Jacobson, K. A., Gao, Z. G., Cherezov, V., and Stevens, R. C. (2011) Structure of an agonist-bound human A2A adenosine receptor. *Science 332*, 322−327.
(54) Park, J. H., Scheerer, P., Hofmann, K. P., Choe, H. W., and Ernst, O. P. (2008) Crystal structure of the ligand-free G-protein-coupled receptor opsin. *Nature 454*, 183−187.
(55) Rosenbaum, D. M., Cherezov, V., Hanson, M. A., Rasmussen, S. G., Thian, F. S., Kobilka, T. S., Choi, H. J., Yao, X. J., Weis, W. I., Stevens, R. C., and Kobilka, B. K. (2007) GPCR engineering yields high-resolution structural insights into β2-adrenergic receptor function. *Science 318*, 1266−1273.
(56) Warne, T., Moukhametzianov, R., Baker, J. G., Nehmé, R., Edwards, P. C., Leslie, A. G. W., Schertler, G. F. X., and Tate, C. G. (2011) The structural basis for agonist and partial agonist action on a β1-adrenergic receptor. *Nature 469*, 241−244.
(57) Heifetz, A., Morris, G. B., Biggin, P. C., Barker, O., Fryatt, T., Bentley, J., Hallett, D., Manikowski, D., Pal, S., Reifegerste, R., Slack, M., and Law, R. (2012) Study of human Orexin-1 and -2 G-protein-coupled receptors with novel and published antagonists by modeling, molecular dynamics simulations, and site-directed mutagenesis. *Biochemistry 51*, 3178−3197.
(58) Warne, T., Serrano-Vega, M. J., Baker, J. G., Moukhametzianov, R., Edwards, P. C., Henderson, R., Leslie, A. G., Tate, C. G., and Schertler, G. F. (2008) Structure of a β1-adrenergic G-protein-coupled receptor. *Nature 454*, 486−491.
(59) Hofmann, S., Frank, R., Hey-Hawkins, E., Beck-Sickinger, A. G., and Schmidt, P. (2013) Manipulating Y receptor subtype activation of short neuropeptide Y analogs by introducing carbaboranes. *Neuropeptides 47*, 59−66.
(60) Mirzadegan, T., Benko, G., Filipek, S., and Palczewski, K. (2003) Sequence analyses of G-protein-coupled receptors: Similarities to rhodopsin. *Biochemistry 42*, 2759−2767.
(61) Surgand, J. S., Rodrigo, J., Kellenberger, E., and Rognan, D. (2006) A chemogenomic analysis of the transmembrane binding cavity of human G-protein-coupled receptors. *Proteins 62*, 509−538.
(62) Venkatakrishnan, A. J., Deupi, X., Lebon, G., Tate, C. G., Schertler, G. F., and Babu, M. M. (2013) Molecular signatures of G-protein-coupled receptors. *Nature 494*, 185−194.